DOI 10.1007/s10891-022-02646-0
Journal of Engineering Physics and Thermophysics, Vol. 95, No. 7, November, 2022

X-RAY STUDY OF THE INTERACTION OF SHOCK WAVES IN STRUCTURAL MATERIALS USING SYNCHROTRON-RADIATION SOURCES

A. O. Kashkarov,[a,b] É. R. Pruuel,[b] K. A. Ten,[b] I. A. Rubtsov,[b,c] E. B. Smirnov,[d,e] and M. A. Biryukova[d,e]

UDC 534.222.2

Conducts of high-speed x-ray experiments on recording the interaction of shock waves in structural materials with synchrotron radiation are discussed using polycarbonate and magnesium as an example. The regimes of reflection of a shock wave from an obstacle, of collision of counter-propagating shock waves in a cylinder, and of descent of a shock wave from the lateral surface of the cylinder toward its center have been implemented. Differences in the mechanics of mass fluxes arising in polycarbonate and magnesium on exposure to shock waves have been shown.

Keywords: *shock waves, structural materials, spall fracture, polycarbonate, magnesium, synchrotron radiation.*

Introduction. Experimental determination of the response of a medium to a shock-wave action or of its shock adiabat is a basis for constructing the equations of state of materials at high pressures and for determining their elastoplastic properties and phase-transition conditions [1, 2]. Results of such experiments can also be supplemented with isotherms obtained under static compression of materials to high pressures [3, 4].

States of a material that are intermediate between its states described by the shock adiabat and the compression isotherm may be determined through the recording of wave interaction in the material. For example, the compression of the material by repeated shock waves is accompanied by the smaller decrease in its internal energy compared to the single shock compression. The material′s state under recompression will be lower than the shock adiabat of single compression, approaching the isotherm. Furthermore, experimental conducts with recompression simplify strongly reaching extremum pressures. The material′s state lying in the region between the shock adiabat and the isotherm may be attained as a result of the interaction of shock waves with unloading waves formed when the shock waves arrive at the material′s boundary.

Determination of the properties of materials of structural elements under shock-wave loads, upon the interaction of the waves in them, is of fundamental importance. External boundaries, joints, internal inhomogeneous inclusions [5], and other technological elements of the structure lead to a multiple reflection and collision of the shock waves in its material, and also to their interaction with unloading waves, which is accompanied by the material′s fracture dependent on the initial geometry of primary shock waves [6].

In the present work, consideration has been given to the possibility of multiframe recording of fast processes using synchrotron-radiation sources [7] to investigate the interaction of waves in structural materials. Experiments were conducted with the reflection of a shock wave from an obstacle, and also with the collision of plane shock waves and with the collision of waves under explosive compression of a cylindrical body from the lateral surface. Polycarbonate PK-ÉT-3.5 and metallic magnesium MA14 were used as the materials under study.

Experimental Stations. Multiframe recording of fast processes using synchrotron radiation (SR) has been implemented at experimental stations of the Siberian Center of Synchrotron and Terahertz Radiation [7] with the use of

[a]Siberian Branch of the Russian Academy of Sciences, 17 Acad. Lavrent′ev Ave., Novosibirsk, 630090, Russia; [b]M. A. Lavrent′ev Institute of Hydrodynamics, Siberian Branch of the Russian Academy of Sciences, 15 Acad. Lavrent′ev Ave., Novosibirsk, 630090, Russia; [c]CCP "SKIF" (Center of Collective Use "Siberian Ring Photon Source"), G. K. Boreskov Institute of Catalysis, Siberian Branch of the Russian Academy of Sciences, 1 Nikolsky Ave., Kol′tsovo, 6300559, Russia; [d]Russian Federal Nuclear Center — Academician E. I. Zababakhin All-Russian Scientific-Research Institute for Technical Physics, 13 Vasil′ev Str., Snezhinsk, 456770, Russia; [e]South Ural State University (National Research University), 70 Lenin Ave., Chelyabinsk, 454080, Russia; email: kashkarov@hydro.nsc.ru. Translated from Inzhenerno-Fizicheskii Zhurnal, Vol. 95, No. 7, pp. 1801–1807, November–December, 2022. Original article submitted December 9, 2021.

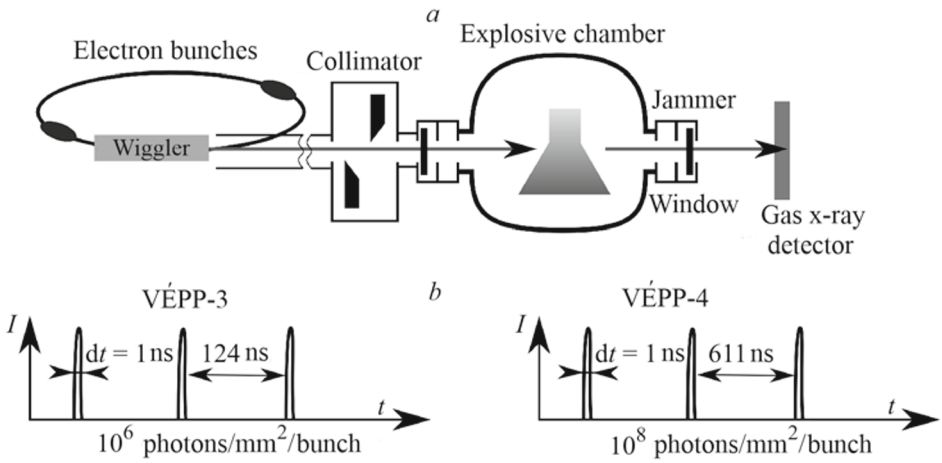

Fig. 1. Diagrams of SR generation (a) and of experimental stations on the VÉPP-3 and VÉPP-4 (b) storage rings.

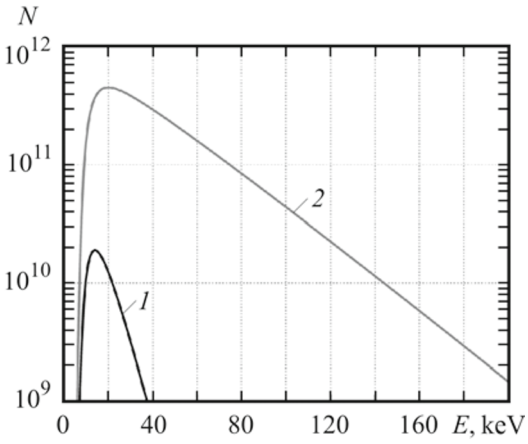

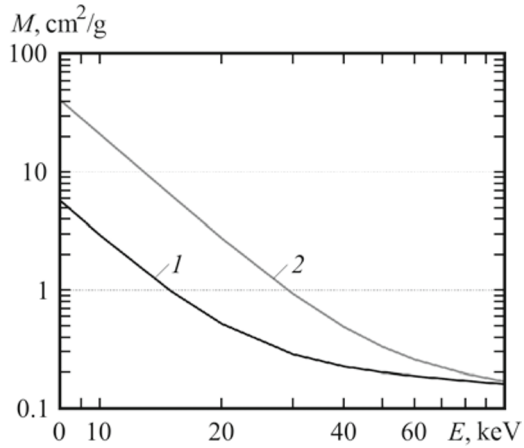

Fig. 2. Spectral characteristics of radiation sources, obtained at the experimental stations on VÉPP-3 (1) and VÉPP-4 (2).

Fig. 3. Mass factors of attenuation of shock waves in polycarbonate (1) and magnesium (2) vs. photon energy.

storage rings of counter-propagating electron-positron beams VÉPP-3/VÉPP-4 of the Institute of Nuclear Physics of the Siberian Branch of the Russian Academy of Sciences.

Diagrams of radiation generation and of the experimental stations are presented in Fig. 1. The duration of x-ray pulses and their period and intensity are determined by the parameters of an accelerator complex and by the structure of a wiggler ensuring the electron motion in an alternating magnetic field to generate an SR beam. The experimental stations "Submicrosecond Diagnostics" and "Extremum State of a Substance" using the VÉPP-3 and VÉPP-4 SR complexes respectively have no fundamental structural differences. The SR beam going out of the wiggler passes through a collimator system and special x-ray transparent explosion-protected windows and is incident onto the specimen under study in the explosive chamber. The radiation transmitted by the specimen carries information on the amount of the substance on the SR beam. Next, the intensity distribution of the SR beam is recorded by the DIMEX fast single-coordinate detector developed at the Institute of Nuclear Physics of the Siberian Branch of the Russian Academy of Sciences specially for studying fast processes [8]. The detector′s recording structure consists of 512 channels arranged along the straight line. Over the period of the SR pulse, the signal at each channel is recorded into its storage cell, and these cells form one frame. The DIMEX detector permits recording 100 frames with a minimum time of 100 ns between the frames. The period of SR pulses in the

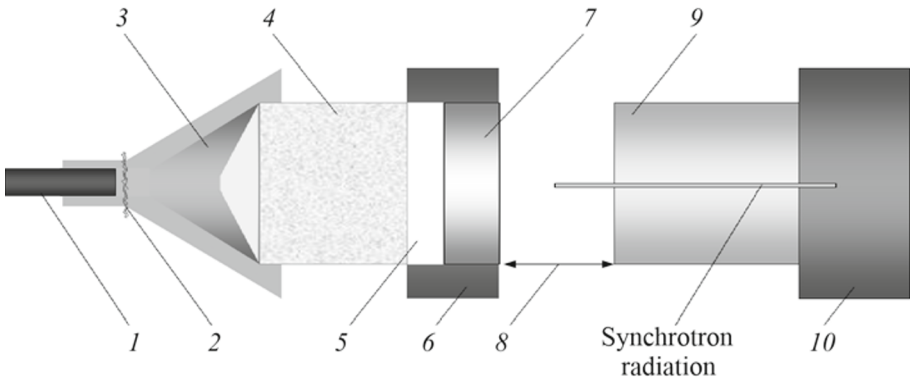

Fig. 4. Scheme of conduct of the experiment on excitation of a shock wave in the specimen: 1) electric detonator; 2) contact sensor; 3) generator of a plane shock wave; 4) active charge; 5) air gap; 6) striker guide; 7) striker; 8) base of flight of the striker; 9) cylindrical specimen; 10) steel obstacle.

experiments at VÉPP-3 was 124 ns, and in the experiments at VÉPP-3, 611 ns, which corresponds to the operating regime of accelerators with two electron bunches rotating in diametrically opposite directions.

Spectral characteristics of the sources are presented in Fig. 2. The mass coefficients of absorption of polycarbonate and magnesium versus the photon energy are plotted in Fig. 3 [9]. The attenuation of radiation when the SR beam is transmitted by the material of the specimen under study depends exponentially on the mass attenuation factor for an assigned photon energy. Therefore, it is specimens of such thickness d, for which the exponent in the radiation-attenuation law $\rho\mu/\rho d$ will be close to unity, that will be optimum from the viewpoint of x-ray radiography. For the VÉPP-3 station, the specimens′ optimum thicknesses determined with allowance for the efficiency of the detector for recording photons of varying energies were 16 mm for polycarbonate and 2 mm for magnesium, and for the VÉPP-4 station, the optimum thickness of the magnesium specimen was about 12 mm now. Thus, at the station "Extremum States of a Substance," we can record shock waves in materials with a high mass coefficient of absorption of x rays, in particular, in magnesium. At the station "Submicron Diagnostics," time resolution is much higher, but it is only materials absorbing x rays weakly in the indicated range of energies, e.g., organic compounds, that are available for investigation. To investigate shock-wave processes in polycarbonate and magnesium, we fabricated specimens with a dimension of 20 mm which was longitudinal with respect to the SR beam. This enabled us to ensure similar parameters of the shock-wave action and a sufficient contrast of x-ray images.

Interaction of the Shock Wave with the Obstacle. Consideration was given to the classical problem on excitation of a shock wave in a specimen by a plate thrown at it (Fig. 4). Detonation products of the active charge threw a plane striker in the direction of a cylindrical specimen. As the striker moved along the base of flight, the SR beam was successively overlapped. In the x-ray photograph of the process, which is presented in Fig. 5, we can see the striker′s boost phase and a portion with a steady-state flight speed. The dynamics of motion of the striker is presented by the narrow dark band. The initial position of the contact boundary is at the zero of the horizontal axis. Upon the collision of the striker with the specimen, the velocities of its end surfaces change. At the instant of collision (6.5 μs), a shock wave is excited in the specimen whose propagation is recorded by additional attenuation of the intensity of transmitted radiation in the region of compression of the specimen behind the shock-wave front. The state of the specimen with recompression is implemented upon the reflection of the shock wave from a steel obstacle at an instant of time of 9 μs from the beginning of recording. Immediately following the collision of the striker with the obstacle, a shock wave propagates over it and the contact boundary moves with a mass velocity. In other words, we have a point on the shock adiabat and the state behind the shock-wave front is quite determined. Next, the shock wave propagating over the material of the striker in the negative direction is reflected by the axial rarefaction wave from its free surface. At the instant the unloading wave breaks the surface of contact of the striker with the specimen, the velocity of this boundary decreases and the characteristic bend is observed at the point $z = 1$ mm. Next, at a depth of about 6.5 m, the axial unloading wave catches up with the shock front in the specimen. Therefore, the shock wave reflected from the obstacle in the specimen is of weak intensity and is imperceptible, in practice. Also, the shock wave is attenuated under the action of lateral unloading which leads to a noticeable curvature of the wave-front′s

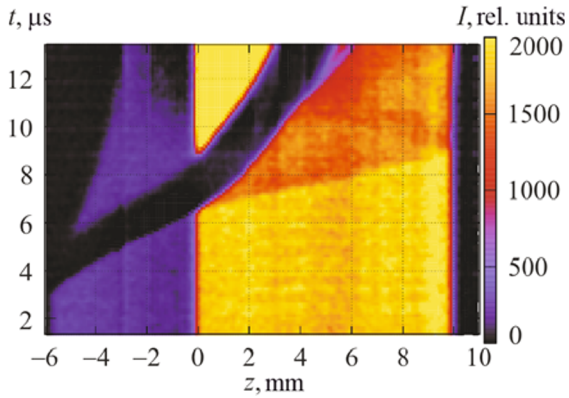

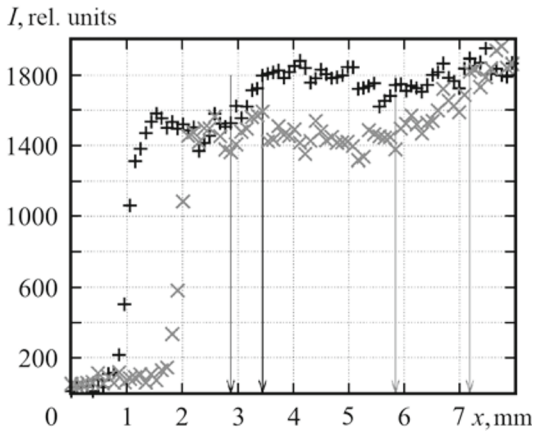

Fig. 5. X-ray photograph of collision of the striker moving from left to right with the specimen.

Fig. 6. Radiation-intensity distribution over the cross section of a cylindrical specimen.

surface. Figure 6 gives individual SR profiles for different positions of the shock-wave front in the specimen under single compression. The front width marked by the lines in the figure reflects its bend on exposure to the lateral unloading wave.

Decrease in the longitudinal dimensions of the specimens under study and increase in the longitudinal dimensions of the strikers make it possible to weaken the influence of unloading waves and to observe higher-intensity waves reflected from the obstacle. Time resolution of the experimental station on the VÉPP-3 storage ring is sufficient for recording the process in the case of short specimens. However, for denser specimens whose investigation is only possible with the VÉPP-4 storage ring, time resolution will a priori be unsatisfactory. Therefore, no experiments in such a formulation were conducted with magnesium.

Collision of Counter-Propagating Shock Waves. A scheme of the experiment on collision of shock waves propagating along the axis of a cylindrical specimen in opposition is given in Fig. 7. Detonation of active charges to the left and right of the specimen under study excite counter-propagating shock waves in it. An x ray photograph of this process for the polycarbonate specimen is presented in Fig. 8a. At an instant of time of 4 μs after the beginning of recording, detonation waves in the active charges are incident onto indicator plates (wide dark bands). Next, the indicator plates move together with the boundaries of the specimen under study. The velocity of contact boundaries of the indicator plates correspond to the mass velocities of the substance of the specimen under study near the plates. The state with recompression is implemented upon the collision of the initial waves at an instant of time of about 5 μs. Subsequent flow is accompanied by the gradual compression of polycarbonate and the decrease in the intensity of transmitted radiation. The copper indicator plates, once the reflected shock waves have arrived at them, bend substantially, which is expressed, in the x-ray photograph, as a noticeable increase in the thickness. This bend is also attributed to the influence of lateral unloading on the shape of the shock-wave front in the specimen. In the experiments with magnesium on the VÉPP-4 storage ring, the structure of flow resulting from the collision of the waves is fundamentally different. It can be seen from Fig. 8b that at the site of collision of the waves, a region appears with a high transmitted-radiation intensity which exceeds the intensity of the SR beam transmitted by the unperturbed specimen. Thus, upon the collision of the shock waves, a spall occurs in the specimen′s central part to form a cavity. Insufficient time resolution of the experimental station on the VÉPP-4 storage ring makes it impossible to resolve a detailed dynamics of interaction of the waves. We can only speak of a certain average velocity of the shock waves before collision, which is 5.6–5.7 mm/μs. The considerable width of the resulting cavity suggests that the spall appears in the longitudinal direction of the cylinder. In other words, tensile stresses ensuring the occurrence of a spall are transverse to the axis of the cylindrical specimen.

Spall fracture occurs, as a rule, after the normal incidence of the shock wave on the body′s free surface, which is accompanied by the occurrence of tensile stress in the unloading wave that is sufficient to destroy the material. In our case shock waves slide over the lateral surface of the cylindrical specimen. Therefore, tensile stresses occurring in the lateral unloading wave are much weaker. The occurrence of a spall in the case of weak tensile stress is attributable to the substantial

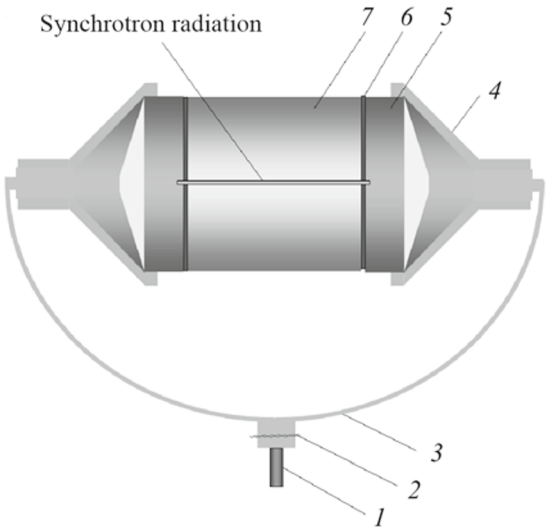

Fig. 7. Scheme of conduct of the experiment on collision of shock waves in the cylindrical specimen: 1) electric detonator; 2) contact sensor; 3) detonation cable; 4) generator of a plane shock wave; 5) active charge; 6) copper indicator plate; 7) cylindrical specimen.

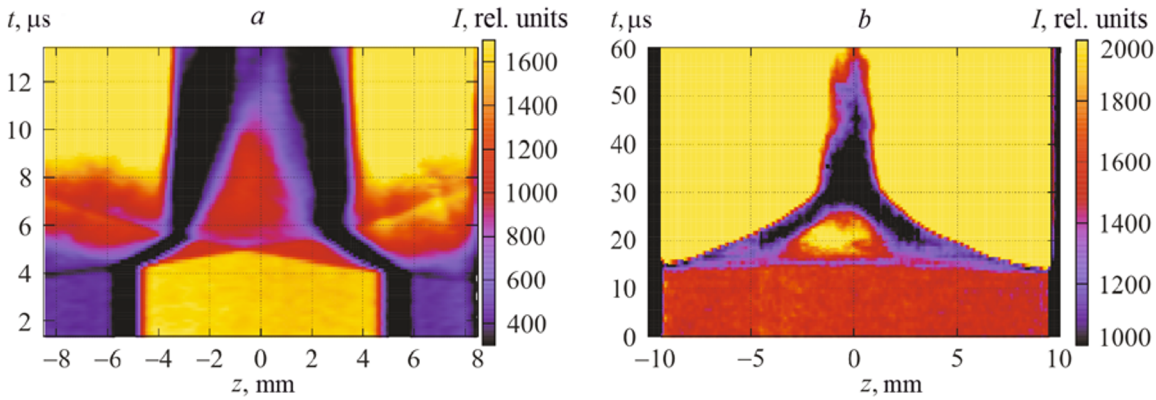

Fig. 8. X-ray photographs of collision of shock waves in polycarbonate (a) and magnesium (b).

decrease in the spall strength of magnesium as the temperature grows [10], which may be considered considerable for the case with recompression. Similar reasoning is also true of polycarbonate specimens, but no spall is observed in the corresponding x-ray photograph.

Cylindrical Cumulation. A diagram of implementation of the compression of the cylinder from the lateral surface is given in Fig. 9. This conduct of the experiment is far, of course, from ideal cylindrical cumulation. However, in the plane of the SR beam, we can observe shock waves converging toward the cylinder′s center. For polycarbonate, the dynamics of the occurring flow is analogous, on the whole, to the previous conduct of the experiment. Upon the collision of primary waves, a state with shock recompression is implemented (Fig. 10a). Next, secondary waves are reflected from the indicator shell and reconverge in the central part of the specimen. The shape of the shock-wave front at this stage is substantially curved now because of the action of lateral unloading from the cylinder′s end. Therefore, in the x-ray photograph, reconverging waves have the shape of broad bands. The curvature of the shock front is also tracked from the broadening of the x-ray shadow from the indicator shell due to its bend. Upon the excitation of shock waves in the polycarbonate specimen, it is in a compressed state throughout the observation period, the intensity of the SR beam in the central part of the region of observation occupied by polycarbonate is lower than the initial values for the unperturbed specimen. A spall of the magnesium specimen under cylindrical compression is observed. The collision of shock waves occurs within approximately 15 μs after the beginning

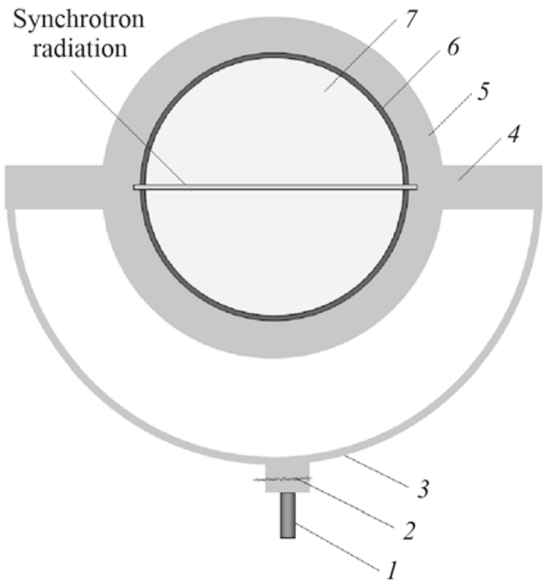

Fig. 9. Scheme of conduct of the experiment on cylindrical cumulation: 1) electric detonator; 2) contact sensor; 3) detonation cable; 4) initiating element; 5) active charge; 6) copper indicator shell; 7) cylindrical specimen.

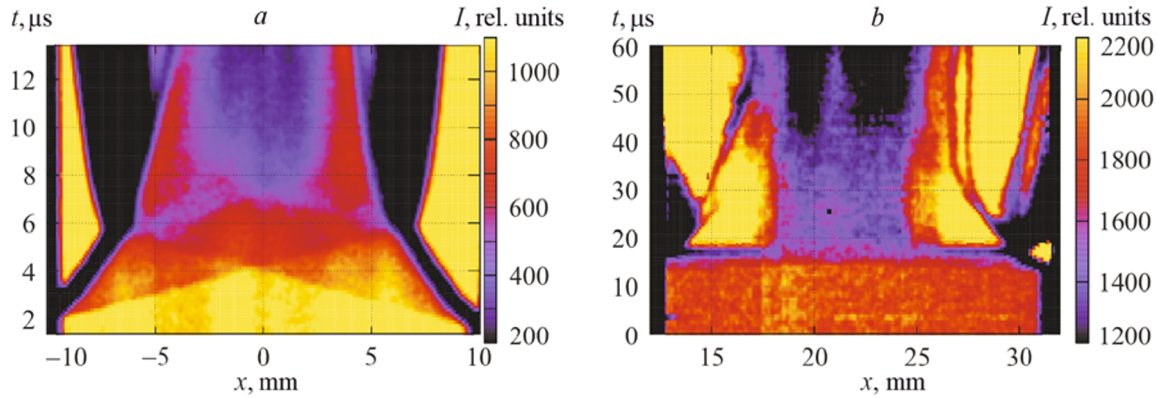

Fig. 10. X-ray photographs of cylindrical compression of polycarbonate (a) and magnesium (b).

of recording of the process. A symmetric spall in the plane of the beam appears near the initiating elements, whereas the specimen′s central part where the primary collision of the shock waves occurs remains fairly dense in this conduct of the experiment. The amount of the substance on the SR beam continues to grow in this region, and the intensity of transmitted radiation, to drop. The spall occurs within approximately 3 μs after recording the reflection of shock waves in this region of the specimen. Therefore, it may be linked to the interaction of unloading waves propagating in a direction transverse to the SR beam from the upper and lower parts of the cylinder. The formation of these waves is most likely to be preceded by the descent and reflection of the shock waves formed during the detonation of the upper and lower parts of the active charge.

Conclusions. Recording fast processes in a material using SR enables us to investigate the mechanics of interaction of shock waves with each other in it and with unloading waves.

In the case of single action of a shock wave excited by the thrown plate on the material the velocity of motion of the shock front and the velocity of mass flow in it are measurable quite accurately and relevant experiments permit obtaining directly points on the shock adiabat of the material. An analysis of experimental data becomes much complicated in observing the interaction of the waves, since here it is necessary to take account of the material′s state ahead of the front of the secondary wave, which will change with time as a result of exposure to unloading waves.

The appearance of a spall in specimens in the experiments with magnesium and its absence in the experiments with polycarbonate is also problematic to explain from just the kinematics of observed shock waves. Differences in the mechanics of mass flows occurring under the shock-wave action on these materials are highly fundamental. For correct interpretation of experimental data on the interaction of waves in them, it is necessary that numerical modeling of the processes be carried out. This will enable us to determine differences in the equations of state of the indicated materials, that are required for reproducing the response experimentally observed in numerical experiment.

Acknowledgment. This work was supported by the grant of the Ministry of Science and Higher Education of the Russian Federation (Project 075-15-2020-781).

NOTATION

E, photon energy; I, radiation intensity; $M = \mu/\rho$, mass factor of attenuation of x rays; N, number of photons; t, time from the beginning of recording x rays by the detector; dt, duration of an x-ray pulse; x and z, coordinates along the cylinder cross section and axis; μ, factor of attenuation (absorption) of x rays per units length; ρ, material′s density.

REFERENCES

1. E. I. Zababakhin, *Some Problems of Explosion Gasdynamics* [in Russian], RFYaTs-VNIITF, Snezhinsk (1997).
2. L. A. Al′tshuler, Use of shock waves in high-pressure physics, *Usp. Fiz. Nauk*, **85**, No. 2, 199–258 (1965).
3. L. Dubrovinsky, N. Dubrovinskaia, E. Bykova, M. Bykov, V. Prakapenka, C. Prescher, K. Glazyrin, H. Liermann, M. Hanfland, M. Ekholm, Q. Feng, L. V. Pourovskii, M. I. Katsnelson, J. M. Wills, and I. A. Abrikosov, The most incompressible metal osmium at static pressures above 750 gigapascals, *Nature*, **525**, No. 7568, 226–229 (2015).
4. Jue Wang, Federica Coppari, Raymond F. Smith, Jon H. Eggert, Amy E. Lazicki, Dayne E. Fratanduono, J. Ryan Rygg, Thomas R. Boehly, Gilbert W. Collins, and Thomas S. Duffy, X-ray diffraction of molybdenum under ramp compression to 1 TPa, *Phys. Rev. B*, **94**, Article ID 104102 (2016).
5. A. E. Kraus, E. I. Kraus, I. I. Shabalin, and A. E. Buzyurkin, Evolution of a shock pulse in a heterogeneous elastoplastic medium, *Prikl. Mekh. Tekh. Fiz*., **62**, No. 3, 147–157 (2021).
6. Z. X. Shen, H. D. Huang, Z. B. Cen, et al., Natural fragmentation behavior of steel cylinders with variable charge geometries under detonation loading, *Combust. Explos. Shock. Waves*, **57**, 246–255 (2021).
7. V. M. Aul′chenko, V. V. Zhulanov, G. N. Kulipanov, K. A. Ten, B. P. Tolochko, and L. I. Shekhtman, Studying fast processes by x-ray diffraction methods at the Siberian Center of Synchrotron and Terahertz Radiation, *Usp. Fiz. Nauk*, **188**, 577–594 (2018).
8. L. I. Shekhtman, V. M. Aulchenko, A. E. Bondar, A. D. Dolgov, V. N. Kudryavtsev, D. M. Nikolenko, P. A. Papushev, E. R. Pruuel, I. A. Rachek, K. A. Ten, V. M. Titov, B. P. Tolochko, V. N. Zhilich, and V. V. Zhulanov, GEM-based detectors for SR imaging and particle tracking, *J. Instrum.*, **7**, Article ID C03021 (2012).
9. M. J. Berger, *NIST XCOM: Photon Cross Sections Database*; https://physics.nist.gov/PhysRefData/Xcom/html/xcom1.html (accessed 20.08.2021).
10. G. I. Kanel, S. V. Razorenov, A. Bogatch, et al., Spall fracture properties of aluminum and magnesium at high temperatures, *J. Appl. Phys*., **9**, Article ID 8310 (1996).